

**ICEWEST-2015 [05<sup>th</sup> - 06<sup>th</sup> Feb 2015]****International Conference on Energy, Water and  
Environmental Science & Technology****PG and Research Department of Chemistry, Presidency College (Autonomous),  
Chennai-600 005, India**

## **Investigation of Photo-Catalytic Activity of TiO<sub>2</sub>- Graphene Composite in Hydrogen Production by Method of Water Splitting**

**<sup>1</sup>Lalith Kumar B\*, <sup>1</sup>Bhoopathy B G, <sup>1</sup>Siddharthan A, <sup>2</sup>Kanmani S****<sup>1</sup>Department of Mechanical Engineering, Anna University, Chennai-600 025, India****<sup>2</sup>Centre for Environmental Studies, Anna University, Chennai-600 025, India**

**Abstract:** TiO<sub>2</sub> nanophotocatalysts were prepared by methods of sol-gel and hydrothermal using same precursor Titanium Tetra Iso-Propoxide. It was observed TiO<sub>2</sub> prepared by hydrothermal gave a higher hydrogen yield which was used in further synthesis of nanocomposites. TiO<sub>2</sub>-graphene (TiO<sub>2</sub>-GR) hybrids were prepared via solvothermal reaction of graphene oxide and TiO<sub>2</sub> using ethanol as solvent. The as-prepared TiO<sub>2</sub>-GR nanocomposites were characterized by X-ray diffraction (XRD), Scanning electron microscopy (SEM), Fourier Transform Infrared (FT-IR) spectroscopy and ultraviolet-visible (UV-vis) diffuse reflectance spectroscopy. The results indicated that TiO<sub>2</sub>-GR nanocomposites possessed enhanced light absorption ability and charge separation efficiency than TiO<sub>2</sub>. The hydrogen evolution from aqueous EDTA and water (30:70) solution under solar-lamp illumination in bench scale tubular reactor (BTR). The optimum mass ratio of GR to TiO<sub>2</sub> in the hybrids was 1 wt. % which produced 1562 μmol h<sup>-1</sup>g<sup>-1</sup> of hydrogen from splitting of water.

**Keywords:** Graphene, TiO<sub>2</sub>, solvothermal reduction, hydrogen production, hydrothermal reduction

### **Introduction**

The increasingly serious energy crisis and the environmental contamination caused by the burning of fossil fuels have led to an aggressive search for renewable and environmental friendly energy resources. Hydrogen energy has been recognized as a potentially significant form of storable and clean energy for the future. Since the discovery of the first water splitting system based on TiO<sub>2</sub> and Pt in 1972 by Fujishima and Honda<sup>1</sup>, many kinds of materials and derivatives have been discovered as photocatalysts for this reaction<sup>2</sup>. Currently, TiO<sub>2</sub> is still one of the most widely used photocatalysts due to its exceptional optical and electronic properties, strong oxidizing power, non-toxicity, chemical stability, and low cost<sup>3</sup>. Typically, photo-excited electron-hole pairs can be generated under the light irradiation with wavelength lower than that corresponding to the band gap energy of TiO<sub>2</sub>. However, the photo-generated electrons and holes in TiO<sub>2</sub> may experience a

rapid recombination, which is one of key factor limiting further improvement of its photocatalytic efficiency<sup>4</sup>. Therefore, one of the most challenging issues on photocatalysis is to overcome the quick recombination of photo-generated electrons and holes.

Several strategies have been employed to improve the photocatalytic performance of TiO<sub>2</sub>, for example, textural design<sup>5</sup>, coupling TiO<sub>2</sub> with metal or other semiconductors<sup>6</sup>, etc. In particular, great interest has been devoted to combining carbon nanomaterials<sup>7</sup>, particularly carbon nanotubes (CNTs)<sup>8</sup>, with TiO<sub>2</sub> to enhance its photocatalytic performance. Graphene (GR) as a new carbon nanomaterial has many exceptional properties, such as high electron mobility, high transparency, flexible structure, and large theoretical specific surface area<sup>9</sup>. Thus, the combination of TiO<sub>2</sub> and graphene is promising to improve the photocatalytic performance of TiO<sub>2</sub>.

Most recently TiO<sub>2</sub>-graphene shows an enhancement of photocatalytic activity for the degradation of methylene blue<sup>10</sup>. TiO<sub>2</sub>-graphene showed higher photocatalytic activity for H<sub>2</sub> evolution from aqueous solution containing Na<sub>2</sub>S and Na<sub>2</sub>SO<sub>3</sub> as sacrificial agents than P25<sup>11</sup>. It has been reported that GO can be reduced to GR by solvothermal reaction of GO in the ethanol solvent<sup>12</sup>. In this paper, photocatalytic activity of TiO<sub>2</sub>-graphene composites prepared by facile solvothermal reactio has been analyzed.

## Experimental Methods

### Preparation of Photocatalyst

Preparation of TiO<sub>2</sub> by Sol-Gel (S-TiO<sub>2</sub>) and hydrothermal method (H-TiO<sub>2</sub>) involves same precursor material Titanium tetra isopropoxide as reported in<sup>13</sup> and<sup>14</sup> respectively. Graphite powder was used for the synthesis of Graphene Oxide (GO) by modified Hummers method<sup>15</sup>. The synthesised GO is reduced to Graphene (GR) along with the TiO<sub>2</sub> Nanoparticles to form the required TiO<sub>2</sub>-X% GR composite, X% = 0.5, 1, 5 and 10, respectively by solvo-thermal reduction<sup>16</sup>.

### Bench-Scale Tubular Photocatalytic Reactor

Tubular reactor was chosen to evaluate the performance of the phtocatalyst. By having the reactor in a cylindrical shape and surrounding it with the lamps (UV and Visible), most of the light energy could be used to activate the catalyst. The schematic picture of the reactor is given in the Fig 1. The working volume of 100 mL was taken with 70 mL water and 30 mL EDTA (Sacrificial reagent). The photocatalyst powder, water and sacrificial reagent were added through the inlet valve of liquid. The air space above the solution in the reactor was flushed with N<sub>2</sub> for 1 h in each experiment. The temperature of the photoreactor (25°C) was maintained by using exhaust fans. The evolved gas was collected in the collection tank by downward displacement of water. The evolved hydrogen was collected and analyzed by Gas Chromatography (Shimadzu - GC 2014ATF: 6890N). The volume of hydrogen was measured at every 15 min interval. Measurements reported are the average of three reading.

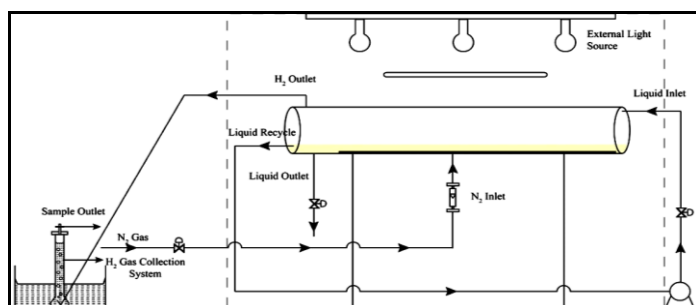


**Fig 1. Schematic Diagram of the Tubular Photocatalytic Reactor**

### Characterization Studies

In order to evaluate the performance of a photocatalyst Fourier Transform Infrared (FTIR) spectra of the samples, recorded using a Bruker FTIR spectrometer (Model IFS 66 v) in the range 4000 – 500 cm<sup>-1</sup> was done for the confirmation of the presence organic group in the powder. Diffuse reflectance (DR) UV-visible spectra were recorded using a CARY 5E UV-Vis-NIR spectrophotometer in the spectral range of 200 – 800 nm to calculate band gap energy. The morphology of sample powders sputtered with gold were seen using SEM (JEOL, JSM 5610LV microscope). X-ray diffractometer (XRD) were recorded using X Pert Pro diffractometer

by Ni-filtered Cu K $\alpha$  radiation ( $\lambda = 1.5418 \text{ \AA}$ ) in the range of  $10 - 90^\circ$  with a step size of  $0.5^\circ$  and the average grain size of the materials was calculated by Scherrer equation.

## Results and Discussion

### Photocatalytic Hydrogen Production

The photocatalytic H<sub>2</sub> evolution (Fig. 2) of H-TiO<sub>2</sub> and S-TiO<sub>2</sub> was found to be 28 ml/h and 30 ml/h respectively. So the activity of H-TiO<sub>2</sub> is found to be higher than that of S-TiO<sub>2</sub>. Therefore H-TiO<sub>2</sub> was selected for further studies to TiO<sub>2</sub>-graphene composite. The hydrogen evolution rate of TiO<sub>2</sub>-X% GR (X% = 0.5, 1, 5 and 10) composite were observed to be 32 ml/h, 35 mL/h, 25 ml/h and 20 ml/h respectively. Among which hydrogen production of TiO<sub>2</sub>-1% GR composite shows 1.2 times higher than that of H-TiO<sub>2</sub> particles. These results were in accordance to Ping *et al.*<sup>16</sup> who reported 12 ml/h with TiO<sub>2</sub>-GR nanocomposite. The role of graphene in TiO<sub>2</sub> and its enhanced evolution of H<sub>2</sub> is described elsewhere<sup>17</sup>. TiO<sub>2</sub> composite with higher percentage of graphene than 1, decreased the hydrogen production due to the "shielding effect"<sup>18</sup>. The gas collected from the inverted jar subjected to gas chromatography technique was confirmed to be hydrogen.

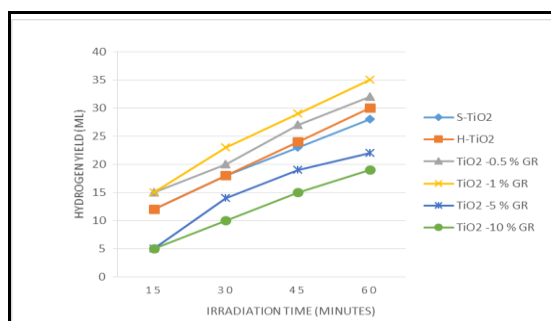


**Fig. 2** The time course of hydrogen production from an aqueous solution with suspended photocatalysts (H-TiO<sub>2</sub>, S-TiO<sub>2</sub> and TiO<sub>2</sub>-X% GR) (0.1 g)

### Characterisation of Synthesised Photocatalysts

#### Molecular Vibrations

The FTIR spectrum of H-TiO<sub>2</sub> is shown in Fig. 3. The peak corresponding to  $2918.18 \text{ cm}^{-1}$  was due to C-H stretching vibration of alkanes. Presence of Oleic acid was confirmed by the vibration at  $1525.20$  and  $1435.27 \text{ cm}^{-1}$  that was used during synthesis. There were bands at about  $1100 \text{ cm}^{-1}$  due to C-O stretching and at  $1371 \text{ cm}^{-1}$  due to CH<sub>2</sub> bending modes of ethanol used for washing. The band close to  $600 \text{ cm}^{-1}$  was assigned to TiO<sub>2</sub> vibration and it was matched with the results reported by Li *et al.*<sup>19</sup>.

The FTIR spectrum of graphene oxide is shown in Fig. 6. The intense broad peak between  $2200$  and  $3700 \text{ cm}^{-1}$  was due to O-H stretching vibration of H<sub>2</sub>O. Presence of H<sub>2</sub>O was confirmed by bending vibration close to  $1630 \text{ cm}^{-1}$ . The peak corresponding to  $3383.34 \text{ cm}^{-1}$  was due to C-H stretching vibration of aromatics. Presence of oxygen bond was confirmed by the vibration at  $1705.12$  and  $1022.38 \text{ cm}^{-1}$  that corresponds to C=O stretch and C-O stretch.

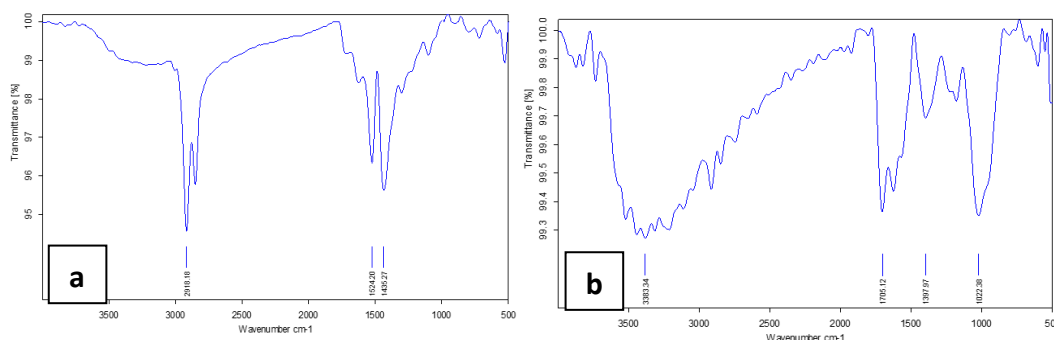


**Fig. 3** a) FTIR spectrum of H-TiO<sub>2</sub> and b) graphene oxide

## Band Gap Energy

The energy band gaps were calculated as 3.18, 3.12 and 2.83 eV corresponding to H-TiO<sub>2</sub>, S-TiO<sub>2</sub> and TiO<sub>2</sub>-1% GR composite respectively from DR-UV spectra shown in Fig. 4. These values are in accordance to 3.2 eV for anatase phase TiO<sub>2</sub> and 2.96 eV for TiO<sub>2</sub>-GR composite Ping Cheng *et al.*<sup>16</sup>. The narrowing of the band gap in the case of TiO<sub>2</sub>-1% GR composite was attributed to the interaction between TiO<sub>2</sub> and GR, similar to that observed for the carbon-doped TiO<sub>2</sub> composites. But on increasing the amount of GR affected the optical property of light absorption for the TiO<sub>2</sub>-GR composite significantly which is in accordance with the hydrogen yield data.

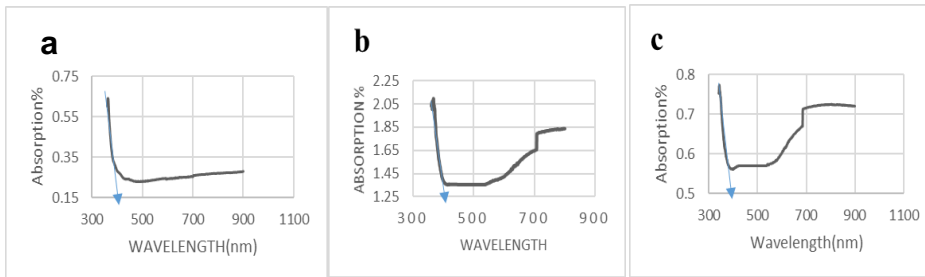


**Fig. 4** DR UV-visible spectra of (a) S-TiO<sub>2</sub>, (b) H-TiO<sub>2</sub> and (c) TiO<sub>2</sub>-1% GR

## Morphology and Particle size

The micrographs of H-TiO<sub>2</sub> and S-TiO<sub>2</sub> powders shown in Fig.5 (a) and (b) respectively were spherical in shape with different sizes. The particles prepared by Sol gel method Fig.5 (a) were fused together which is not in the case of particles prepared by Hydrothermal where individual separate spherical particles were seen in Fig.5 (b). The average particle size of H-TiO<sub>2</sub> and S-TiO<sub>2</sub> is found to be in the range of 100-300 nm and 300-500 nm using image j software. Flake like structures of Graphene were seen in Fig. 5 (c). The morphology of TiO<sub>2</sub>-Graphene composite shown in Fig. 5 (d) was similar to that of H-TiO<sub>2</sub>. This is because of the use of H-TiO<sub>2</sub> in the synthesis of TiO<sub>2</sub>-Graphene composite. But the powders in TiO<sub>2</sub>-Graphene composite were fused together with the graphene and forms island like morphology.

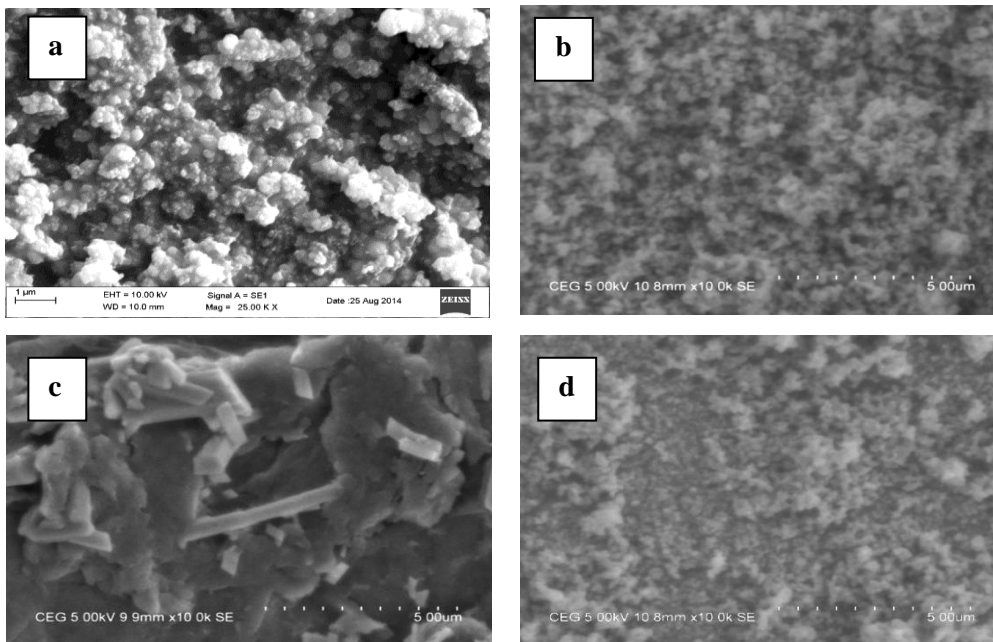


**Fig. 5** SEM micrographs of (a) H- TiO<sub>2</sub>, (b) S-TiO<sub>2</sub>, (c) Graphene and (d) TiO<sub>2</sub>- Graphene composite

## Grain size

The XRD pattern of graphene in Fig. 6 (a) showed one intense peak at 11.32° corresponding to (002) plane of Graphene Oxide and a broad peak between 15° and 30° corresponding to graphene (020) plane which is in accordance with Li *et al.*<sup>19</sup>. In general carbon (002) standard peak will be observed at 26°. Because of the single layer of carbon rings in the graphene makes the XRD peak at 26° broader.

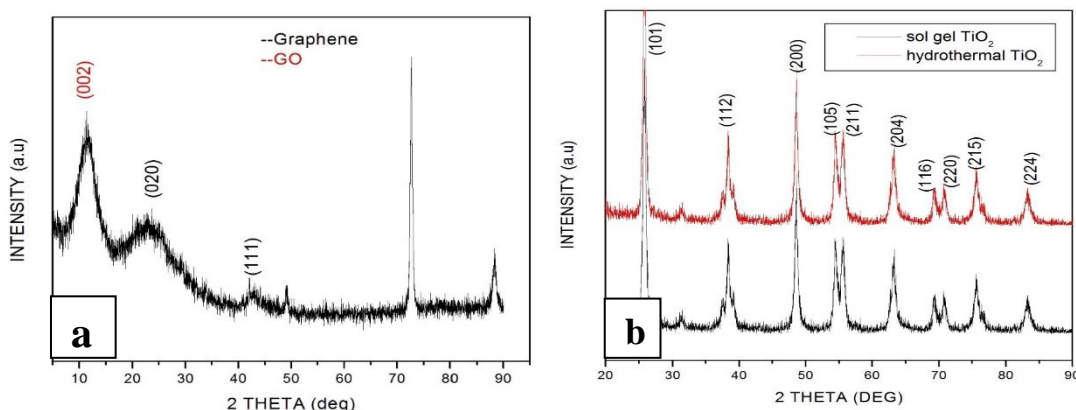


**Fig. 6 XRD pattern of (a) Graphene and (b) H-TiO<sub>2</sub> and S-TiO<sub>2</sub>**

The XRD patterns of H-TiO<sub>2</sub> and S-TiO<sub>2</sub> are shown in Fig. 6 (b). The peaks were very much sharp and not broadened enough to be nanoparticles (i.e. 1-100 nm). Both XRD patterns were similar and they matched with the anatase form. The peaks were indexed using JCPDS Card No. 21-1272. The average crystal size of H-TiO<sub>2</sub> and S-TiO<sub>2</sub>, calculated by Scherrer Equation were 20.39 nm and 16.13 nm respectively using peaks corresponding to (xxx) plane.

## Conclusions

TiO<sub>2</sub> powders synthesized by hydrothermal method gave a higher hydrogen production than TiO<sub>2</sub> prepared by sol gel method. The hydrogen yield of TiO<sub>2</sub>-Graphene composites was maximum at 1% GR which shows 1.2 times higher than that of H-TiO<sub>2</sub> particles and then decreased with increase in graphene percentage than 1%. Results obtained from this research indicated that the synthesized novel solar UV light responsive nanocomposite TiO<sub>2</sub>-1% GR effectively decomposed the H<sub>2</sub>O in an alkaline solution along with generation of clean H<sub>2</sub>.

## References

1. Fujishima A. Electrochemical photolysis of water at a semiconductor electrode. *Nature.*, 1972, 238: 37-38.
2. Ashokkumar M. An overview on semiconductor particulate systems for photoproduction of hydrogen. *Int J Hydrogen Energy.*, 1998, 23:427-38.
3. Huang BS, Wey MY. Properties and H<sub>2</sub> production ability of Pt photodeposited on the anatase phase transition of nitrogen doped titanium dioxide. *Int J Hydrogen Energy.*, 2011, 36:9479-86.
4. Bak T, Nowotny J, Rekas M, Sorrell C. Photo-electrochemical hydrogen generation from water using solar energy. Materials-related aspects. *Int J Hydrogen Energy.*, 2002, 27: 991-1022.
5. Tomkiewicz M. Scaling properties in photocatalysis. *Catal Today.*, 2000, 58:115-23.
6. Tryba B, Tsumura T, Janus M, Morawski AW, Inagaki M. Carbon-coated anatase: adsorption and decomposition of phenol in water. *Appl Catal B.*, 2004, 50:177-83.
7. Inagaki M, Kojin F, Tryba B, Toyoda M. Carbon coated anatase: the role of the carbon layer for photocatalytic performance. *Carbon.*, 2005, 43:1652-9.
8. Woan K, Pyrgiotakis G, Sigmund W. Photocatalytic carbon-nanotube-TiO<sub>2</sub> composites. *Adv Mater.*, 2009, 21: 2233-9.
9. Nair RR, Blake P, Grigorenko AN, Novoselov KS, Booth TJ, Stauber T. Fine structure constant defines visual transparency of graphene. *Science.*, 2008, 320:1308.
10. Zhang H, Lv XJ, Li YM, Wang Y, Li JH. P25-graphene composite as a high performance photocatalyst. *ACS Nano.*, 2010, 4:380-6.
11. Zhang XY, Li HP, Cui XL, Lin YH. Graphene/TiO<sub>2</sub> nanocomposites: synthesis, characterization and application in hydrogen evolution from water photocatalytic splitting. *J Mater Chem*, 2010, 20:2801-6.
12. Nethravathi C, Rajamathi M. Chemically modified graphene sheets produced by the solvothermal reduction of colloidal dispersions of graphite oxide. *Carbon.*, 2008, 46:1994-8.

13. Kavitha Thangavelu , Rajendran Annamalai, Durairajan Arulnandhi. Preparation and Characterization of Nanosized TiO<sub>2</sub> Powder by Sol-Gel Precipitation Route. International Journal of Emerging Technology and Advanced Engineering., 2013; 3; 636-639.
14. Qifeng Chen. Anatase TiO<sub>2</sub> Mesocrystals Enclosed by (001) and (101) Facets: Synergistic Effects between Ti<sup>3+</sup> and Facets for Their Photocatalytic Performance. European journal., 10.1002/chem.201201178
15. Gaoquan Shi. An improved Hummers method for eco-friendly synthesis of graphene oxide. CARBON., 2013, 64 : 225 –229.
16. Ping Cheng. TiO<sub>2</sub>-graphene nanocomposites for photocatalytic hydrogen production from splitting water. international journal of hydrogen energy., 2012, 37: 2224-2230.
17. Wang X. Transparent, Conductive graphene electrodes for dye-sensitized solar cells. Nano Letters., 2008, 8: 323-7.
18. Yu JG. Enhanced photocatalytic activity of mesoporous TiO<sub>2</sub> aggregates by embedding carbon nanotubes as electron-transfer channel. Phys Chem Chem Phys., 2011, 13: 3491-501.
19. Li et al. Preparation and electrochemical performance for methanol oxidation of pt/graphene nanocomposites. Electrochemistry Communications.,2009, 11 : 846–849.

\*\*\*\*\*